

## Modeling of linear optical controlled-z quantum gate with dimensional errors of passive components

F. D. Kiselev<sup>1,2</sup>, E. Y. Samsonov<sup>1</sup>, A. V. Gleim<sup>1</sup>

<sup>1</sup>ITMO University, Kronverkskiy, 49, St. Petersburg, 197101, Russia

<sup>2</sup>Corning Research & Development Corporation, Corning, NY

kiselevfd@corning.com, eduard.s1994@list.ru, aglejm@yandex.ru

PACS 42.00.00, 42.82.Gw

DOI 10.17586/2220-8054-2019-10-6-627-631

Linear optical quantum computing can be realized using photonic integrate circuits (PICs). It is advantageous in comparison to other physical implementations of quantum computing due to simplicity of qubit encoding using photons and low decoherence times. Passive components like beamsplitters and phaseshifters are key elements for such PICs. In this article, we present modeling of linear optical controlled-Z gate with imperfections of beamsplitters and phaseshifters taken into account. Results showed that errors occur which cannot be detected by projection measurements and post-selection proposed by Knill, Laflamme and Milburn. We studied how these errors and success probability changes with the increase of dimensional errors using Monte-Carlo simulation. The obtained results can be used for design and calibration stages of chip manufacturing.

**Keywords:** quantum computing, linear optics.

*Received:* 2 April 2019

*Revised:* 6 November 2019

*Final revision:* 12 November 2019

### 1. Introduction

Quantum computing is a paradigm which considers usage of quantum mechanical effects in computation allowing massive parallelism and overall superiority relative to classical computing for many important problems [1]. Quantum computing operates with unitary operations, called gates, which are building blocks of any quantum algorithm. Controlled-Z gate (or CZ-gate in short) is one of the basic 2-qubit gates which are considered to be a part of a universal set [2]. This is thus required for a quantum computer to be able to perform any unitary operation. For example, it is presented in Grover's [3] and Shor's [4] algorithms. There are several physical platforms for implementation of quantum computing. The most popular one being evaluated by IBM that uses qubits based on superconductivity [5]. In this paper, we consider linear optical quantum computing (LOQC). Linear optical implementation of quantum computing has many advantages over superconducting alternatives, including: significantly longer decoherence times, simplicity of qubit encoding, as well as the benefits of using integrated photonic circuits as a physical platform. Typical LOQC chip is constructed from beamsplitters (or directional couplers) and phaseshifters. It was shown in [6] that any unitary operation can be constructed only with certain amount of these elements. Such simplicity might be attractive, however there are many issues in LOQC that need to be addressed. One of the main issues with linear optical quantum computing is probabilistic behavior of many-qubit gates [7]. It appears that every linear optical gate that has been proposed is capable of performing supposed operation only with certain probability due to the variation of basis states in the system which do not correspond to the right operation. Knill, Laflamme and Milburn [7] proposed using ancilla channels and projection measurements on them to force the system of the gate to collapse into a specific set of basis states, one of them corresponding to a desired operation. Such an approach does not solve the problem of non-determinacy, but at least gives us an ability to monitor whether the operation was performed correctly or not. Another feature was proposed by the same authors to make near-deterministic operations by using multiple gates acting on the entangled set of qubits and using a teleportation protocol to extract the successfully applied gate and feed it forward to the computation. One can note that both approaches make the system more complex, introducing a significant number of optical elements and increasing number of channels. Other issues include: probabilistic generation of single-photons, coupling losses, inefficiency of single-photon detectors, and different optical losses occurring inside the scheme. Most popular designs for LOQC systems use photonic integrated circuits (PIC's), as they enable good dimensional stability, compact sizes and integrability [8]. These circuits could be manufactured using ion exchange technology as was shown in [9]. But the most popular approach is to use silicon nanowires, as they have much more compact nanoscale sizes and also more components can be integrated in such chip [10]. However, there are manufacturing tolerances of such systems which

need to be taken into account before designing any practical system. Even if a controllable Mach-Zehnder interferometer is used to mitigate these issues, it is important to know to what point MZIs need to be calibrated [11]. The topic of a quantum algorithm's performance on a real device was studied in [12], where the authors used IBM's superconducting quantum processor. In this paper, we present a modeling approach and results for simulation of linear optical CZ-gate with dimensional imperfections of its passive components – beamsplitters and phaseshifters.

## 2. Modeling approach

A conventional approach to qubit encoding with photons is called dual-rail encoding. This means that a qubit's state depends on the superposition of photon being in two optical modes. These modes can be spatial, polarization or even temporal. The KLM protocol considers spatial optical modes, and thus, our CZ-gate uses two optical channels to represent each of the 2 qubits. This correspondence can be written as

$$|0\rangle = |1\rangle_1 \otimes |0\rangle_2 = |1_1 0_2\rangle,$$

$$|1\rangle = |0\rangle_1 \otimes |1\rangle_2 = |0_1 1_2\rangle,$$

where left part represents qubit states, but the middle and right parts represent two different notations of a single photon existing in one of the two optical modes. The optical scheme of CZ-gate is taken from [7] and presented in Fig. 1. It consists of 4 logical optical modes, two of which are coupled to 4 ancilla modes. A single logical mode coupled to two ancilla ones with additional single-photon source and detectors form the so called nonlinear-sign (NS) gate (Fig. 2) which performs the following operation on Fock basis states:

$$|\Psi_{in}\rangle = \alpha|0\rangle + \beta|1\rangle + \gamma|2\rangle \rightarrow |\Psi_{out}\rangle = \alpha|0\rangle + \beta|1\rangle - \gamma|2\rangle.$$

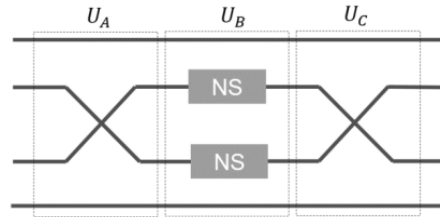


FIG. 1. Schematic of a KLM CZ-gate with 4 ancilla channels (right) and its representative matrix calculated using our modeling approach (left)

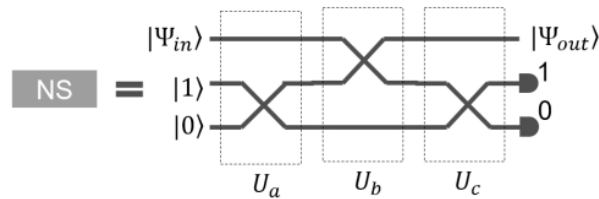


FIG. 2. Schematic of the nonlinear sign-flip gate consisting of one logical and two ancilla channels

The NS gate applies successfully when single photon is measured in the respective ancilla channel. Probability of that happening in the ideal case is  $1/4$ , which makes success probability of CZ gate equal to  $1/16$ . In our model, we divide the gate into parts each of which can be described by a single time-independent Hamiltonian. Passive components within these parts are described by following Hamiltonians:

$$\hat{H}_{BS} = \hat{a}_i^\dagger \hat{a}_j + \hat{a}_j^\dagger \hat{a}_i, \quad \hat{H}_{PS} = \hat{a}_i^\dagger \hat{a}_i,$$

where  $i, j$  are numbers of optical modes and  $\hat{a}_i$  are mode operators which act as annihilation operator on the channel with respective number. Transformation operators are then calculated via matrix exponential:

$$U = \exp(i\hat{H}_{BS/PS}z),$$

where propagation length  $z$  represents the effective interaction length of the directional coupler or the phase shift of the phaseshifter. Thus, dimensional errors can be introduced directly into equation shown above as random displacement  $\Delta z$ . We used Quantum Toolbox in Python (QuTiP) to setup and calculate our model.

In order to compute our model efficiently, we decided to split it into two steps. The first step is solving NS gate, which consists of 3 channels and operates with 3 photons. The two-photon state is taken as an input for the logical channel and an additional photon is taken as an input for the first ancilla channel. The important thing in this part is application of projection measurement operator, which corresponds to a successful performance of this gate:

$$P_{10} = (I \otimes |1\rangle\langle 1| \otimes |0\rangle\langle 0|).$$

The success probability of the NS gate can then be calculated as a norm of the output wave function. Second step is to solve CZ-gate itself. Here, we use matrices of NS-gates extracted from the previous calculation using partial trace. Two matrices are then included into a tensor multiplication, forming a transformation operator acting on 4 logical channels of CZ gate:

$$U_B = (I \otimes U_{NS}^1 \otimes U_{NS}^1 \otimes I).$$

The calculated CZ-gate is then applied to an input state of two photons being launched into second and third logical channels which logically correspond to  $|11\rangle$  state. Here, we lay out the correspondence between optical basis states and computational ones. Subsequently, we will only use computational notations:

$$\begin{aligned} |00\rangle &= |1_1 0_2 0_3 1_4\rangle, \\ |10\rangle &= |0_1 1_2 0_3 1_4\rangle, \\ |01\rangle &= |1_1 0_2 1_3 0_4\rangle, \\ |11\rangle &= |0_1 1_2 1_3 0_4\rangle. \end{aligned}$$

The success probability of this gate is calculated as multiplication of success probabilities of NS gates. Dimensions of these two problems are 3 channels, 3 photons and 4 channels, 2 photons, respectively. Such an approach appears to be significantly more efficient in comparison with the more straightforward approach that does not separate the problem and deals with 8 channels and 5 photons. One should note that we were able to divide the problem due to the presence of projection measurements in the NS gate. Projection measurement destroys entanglement between logical and ancilla channels. Thus, we can apply operation of partial trace without losing any important information.

As it was stated before, we can apply dimensional error of the phaseshifter or a beamsplitter as a random displacement of the propagation length. It is pretty straightforward for the characterization of phase shift. For the beamsplitter, however, it is more convenient to use value of splitting coefficient. Splitting coefficient of a beamsplitter is a ratio between input power and output power of the opposite channel. It can be calculated as:

$$C = \sin^2 \left( \frac{\pi L_{int}}{2 l_c} \right),$$

where,  $L_{int}$  is an effective interaction length which in our case correspond to the value of  $z$ ,  $l_c$  is the coupling length which corresponds to a values of interaction length required to fully couple light from one channel to another. The coupling length can be calculated for a given waveguide structure using overlap integrals and finite element method. In the initial simulation, we randomly choose errors for each component within boundaries of  $\pm 0.05$  for splitting coefficient and  $\pm \pi/40$  for phase shift. These errors correspond to various dimensional errors which can occur in the manufacturing process of the component. For example silicon nitride-based directional couplers have such errors if the 400 nm separation between waveguides in the interaction region is displaced by 25 nm [13]. Other imperfections may occur in a value of interaction length and in a cross-section geometry of the waveguide. To observe the impact of these imperfections on the gate performance and to understand what it means, we considered diagonal elements of output wavefunction partial traces which basically gives us photon number distribution at given channels. In an ideal case, we should measure exactly one photon in the second and third channels for the input state  $|11\rangle$ . One can see in Fig. 3 that in the case of a dimensionally imperfect chip we are getting non-zero probabilities of 0 and 2 photons being measured at the output of respective logical modes. We want to point out that these errors occur if the projection measurement in both NS gates were successful thus they are not detectable by KLM-protocol and cannot be separated from the computation without some additional measures. In the next section of this article we investigate how this error depends on the amplitude of these imperfections.

### 3. Monte-Carlo simulations

Since dimensional errors of passive components are random in nature, we use the Monte-Carlo approach to study its effect on the performance of CZ-gate. At each step, we choose boundaries for splitting coefficient and phase errors. These boundaries are called dimensional error rate and defined by the relative change of splitting coefficient and phase shift with 0.5 and  $\pi/2$  as references respectively. Then we run 1000 iterations randomly choosing errors of passive

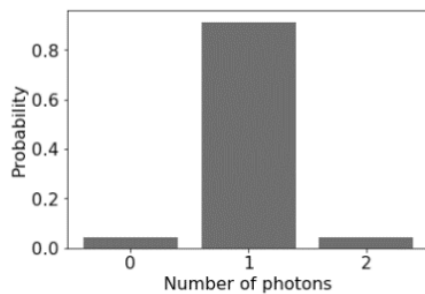


FIG. 3. Photon number probability distribution at the output of  $2^{nd}$  and  $3^{rd}$  logical optical modes. Probabilities at 0 and 2 photons correspond to the error caused by dimensional imperfections within  $\pm 0.05$  for splitting coefficient and  $\pm \pi/40$  phase shift

components within defined boundaries. At the output we observe mean and maximum probability of error which is calculated as

$$P_{err} = 1 - \frac{1}{P_{succ}} \langle 11 | \rho_{out} | 11 \rangle,$$

where  $\rho_{out}$  is the density matrix of the output state and  $P_{succ}$  is the success probability of CZ gate calculated as multiplication of success probabilities of two NS gates. This is basically probability of not measuring  $|11\rangle$  state at the output even if both projection measurements were successful. It also corresponds to an imperfect photon number distribution showed in Fig. 3. Fig. 4 shows how probability of error grows with dimensional error rate being increased. One can readily see that the growth is nonlinear. Maximum error represents worst case scenario and it grows much faster than the mean error. This indicates that statistics of error probabilities spreads with the increase of error rate. From that, we conclude that larger dimensional errors not only introduce larger possibility of false computation, but also make performance of the chip less predictable. This also means that large enough dimensional errors won't allow us to separate its impact from other possible flaws in the experiment, unless dimensions of the device will be rigorously measured to calculate its exact impact with respect to our model, which could be complicated.

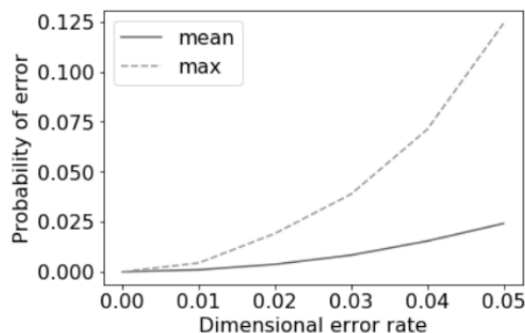


FIG. 4. Mean and maximum error probabilities obtained from Monte-Carlo simulation for different rates of dimensional errors

Another interesting thing to determine is the success probability of the gate (Fig. 5). Unlike the error probability, its mean value doesn't show a continuous decrease. However, maximum and minimum values spread around the ideal  $1/16$ . This again impacts the performance predictability of the device.

#### 4. Conclusion

We proposed a modeling approach for KLM CZ-gate simulation with random dimensional imperfections of passive components taken into account. As a result, we observed errors – non-zero probabilities of 0 and 2 photons being measured at the output of optical modes which correspond to the basis state of  $|11\rangle$ . These errors cannot be detected by projection measurements. We used Monte-Carlo simulations to calculate mean and maximum error probabilities depending on the rate of dimensional errors. Our results show that maximum probability, which represents the worst case scenario for a given error rate, grows much faster than the mean one. Additionally, the success probability, which corresponds to a certain result of projection measurement, can significantly deviate from the ideal case in the presence

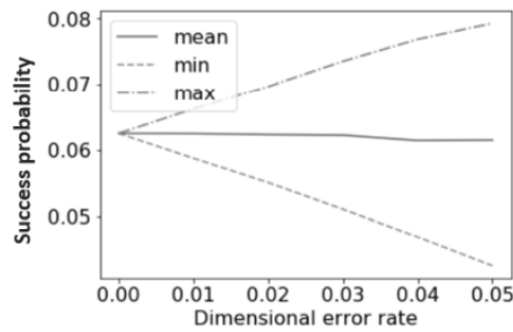


FIG. 5. Mean, minimum and maximum success probabilities of CZ-gate obtained from Monte-Carlo simulation for different rates of dimensional errors

of imperfections. These effects should be taken into account in the design stage of schemes with a large number of such gates. The proposed model can be used for calculation of gate matrix and then applied to performance simulation of quantum computational schemes based on LOQC.

## References

- [1] DiVincenzo D.P. Quantum computation. *Science*, 1995, **270** 5234), P. 255–261.
- [2] Barenco A., Bennett C.H., et al. Elementary gates for quantum computation. *Phys. Rev. A*, 1995, **52**, P. 3457–3467
- [3] Grover L.K. A fast quantum mechanical algorithm for database search. *Proceedings of Annual ACM symposium on Theory of Computing*, Philadelphia, Pennsylvania, USA, ACM, 1996, P. 212–219.
- [4] Politi A., Matthews C.J., OBrien J. Shor's Quantum Factoring Algorithm on a Photonic Chip. *Science*, 2009, **325** (5945), P. 255–261.
- [5] Devoret M.H., Schoelkopf R.J. Superconducting Circuits for Quantum Information: An Outlook. *Science*, 2013, **339** (6124), P. 1169–1174.
- [6] Reck M., Zeilinger A., Bernstein H.J., Bertani P. Experimental realization of any discrete unitary operator. *Phys. Rev. Lett.*, 1994, **73** (1) P. 58–61.
- [7] Knill E., Laflamme R., Milburn G.J. A scheme for efficient quantum computation with linear optics. *Nature*, 2001, **409**, P. 46–52.
- [8] Silverstone J.W., Bonneau D., OBrien J., Thompson M.G., Silicon Quantum Photonics. *IEEE Journal of Selected Topics in Quantum Electronics*, 2016, **22** (6), P. 390–402.
- [9] Gerasimenko V., Gerasimenko N., et al. Numerical modeling of ion exchange waveguide for the tasks of quantum computations. *Nanosystems: Physics, Chemistry, Mathematics*, 2019, **10** (2), P. 147–153.
- [10] Sun J., Timurdogan E., et al. Large-scale nanophotonic phased array. *Nature*, 2013, **493**, P. 195–199.
- [11] Miller D.A. Perfect optics with imperfect components. *Optica*, 2015, **2** (8), P. 747–750.
- [12] Gubaidullina K.V., Chivilikhin S.A. Stability of Grover's algorithm in respect to perturbations in quantum circuit. *Nanosystems: Physics, Chemistry, Mathematics*, 2017, **8** (2), P. 243–246.
- [13] Poot M., Schuck C., et al. Design and characterization of integrated components for SiN photonic quantum circuits. *Optics Express*, 2016, **24** (7), P. 6843–6860.